Journal of New Materials for Electrochemical Systems 13, 21-27 (2010)

Evaluation of Colloidal Pd and Pd-alloys as Anode Electrocatalysts for Direct Borohydride Fuel Cells Applications

M.H. Atwan[1,*], E.L. Gyenge[2], and D.O. Northwood[3,*]

[1]General Motors R&D Technical Center (for Trison Engineering), Warren, MI 48090, USA
[2]Chemical and Biological Eng., the University of British Colombia, Vancouver, BC, V6T 1Z4, Canada
[3]Mechanical, Auto, and Materials Eng., University of Windsor, Windsor, N9B 3P4, Canada

Received: July 29, 2009, Accepted: August 04, 2009

Abstract: *Borohydride oxidation on supported Pd and Pd-alloy nano-electrocatalysts (Pd, Pd-Ir, Pd-Ni, Pd-Au, and Pd-Ag) prepared by a modified Bönneman method has been investigated using cyclic voltammetry (CV), rotating disk electrode (RDE) voltammetry, and single fuel cell test station. Electrochemical parameters, such as Tafel slopes, exchange current densities, oxidation peak potentials, and fuel cell performance, have been determined. The electrochemical parameters impact on the cell performance is considered as important as that of the operating conditions. The influences of temperature, and fuel and oxidant flow rates, on the fuel cell performance were also evaluated.*

The current density of the borohydride fuel cell increases with increase in temperature for all investigated electrocatalysts. The increase in current density with increase in fuel flow rate was not as high as expected within the investigated flow rate range. This is in a good agreement with RDE results. A fuel cell employing Pd-Ir as the anode catalyst and operated at a cell voltage of 0.5 V, can give a current density of 50 mA cm^{-2} at 298 K, while the same catalyst and at same cell voltage can give 110 mA cm^{-2} at 333 K.

Keywords: borohydride fuel cells, colloidal metals, electrocatalysis.

1. INTRODUCTION

Among the fuel cell systems under demonstration and development, hydrogen-based fuel cells are the most developed. Safety, storage, and supply of this flammable gas are still questionable [1]. As alternative fuel that is, safe, readily available, easily transported, and oxidized rapidly at a negative potential, is required. Methanol has been widely investigated as an alternative fuel, but a low activity, poisoning, and crossover have been the main hurdles preventing methanol from being used practically [2].

Another solution is sodium borohydride. Suda et. al. [3] in 2005 and De Leon et. al. [4] in 2006 have published very extensive reviews of borohydride fuel cells. The direct borohydride fuel cell is the most attractive of the direct liquid fuel cells for utilization in portable applications, since it has no catalytic poisoning and less crossover problems than the methanol and formic acid systems, and is more environmentally benign than the hydrazine system. Moreover, using air as an oxygen source, such a fuel cell has a theoretical voltage of 1.64 V [2]. This is a significantly higher cell voltage compared to the methanol, formic acid and hydrazine systems, with theoretical cell voltages of 1.24, 1.45, and 1.56 V, respectively [2, 5, 6].

The direct oxidation reactions of borohydride are:

Anode:

$$BH_4^- + 8OH^- \rightarrow BO_2^- + 6H_2O + 8e^- \qquad E^o = -1.24V_{SHE} \quad (1)$$

Cathode:

$$2O_2 + 4H_2O + 8e^- \rightarrow 8OH^- \qquad E^o = 0.41V_{SHE} \quad (2)$$

Overall:

$$BH_4^- + 2O_2 \rightarrow BO_2^- + 2H_2O \qquad E^o_{cell} = 1.64V \quad (3)$$

For direct borohydride fuel cell applications, a variety of different materials have been studied as anode catalysts: nickel boride, palladium, and platinum powders [7]; 97% Au -3% Pt [8]; a Zr-Ni-alloy [9, 10]; and supported and unsupported Pt [11].

In this study, the effect of alloying Pd with Ir, Ni, Au, and Ag on the electroactivity towards the oxidation of BH_4^- of colloidal Pd and Pd-alloy nano-electrocatalysts, supported on Vulcan XC72R C-black and prepared using the modified Bönneman method, has

*To whom correspondence should be addressed: Email: dnorthwo@uwindsor.ca and mohammed.atwan@gm.com

been carefully investigated using a variety of fundamental electrochemical techniques, including cyclic voltammetry (CV), rotating disk electrode (RDE) voltammetry, and a single fuel cell test station. This study complements our previous work on Pt and Pt-alloys [12], Au and Au-alloys [13], and Ag and Ag-alloys [14, 15] nano-electro catalysts.

2. EXPERIMENTAL

2.1. Colloidal metal Preparation Technique

The colloidal metals were prepared using a modified Bönneman method [16] as described by Götz and Wendt [17]. The colloidal metals were prepared with a 20 %wt load on Vulcan XC72R support (L. V. LAMOS Limited). The alloying ratio was 1:1 atomic. A dry nitrogen glove box atmosphere was used to handle and weigh the reactants. The reactions were performed in a dry nitrogen atmosphere using Schlenk flasks and nitrogen lines.

Stoichiometric amounts of 1M of tetrabutylammonium chloride ($C_{16}H_{36}ClN$) in tetrahydrofuran (THF) (Sigma-Aldrich, >99% Anhydrous) and 1M of Lithium triethylhydroborate ($C_6H_{16}BLi$) in THF (Sigma-Aldrich, 1 M in THF, Anhydrous) were mixed to obtain a solution of 0.5M of tetrabutylammoniumtriethyl hydroborate, $N(C_{16}H_{36})4[Bet_3H]$. LiCl was removed by passing the reaction products solution through a D-4 glass frit. A 50% excess (3, 7.5, 6, 7.5 and 4.5 ml) of 0.5M of tetrabutylammoniumtriethyl hydroborate, $N(C_{16}H_{36})_4[Bet_3H]$, was added dropwise over a period of 1 h at 296 K to a stirred suspensions of anhydrous salts of $PdCl_2$ (STREM Chemical, Inc., 99.9%, Anhydrous) (0.0886 g, 0.5 mmol), $PdCl_2$ (0.0886 g, 0.5 mmol) and $IrCl_3$ (STREM Chemical, Inc., Ir% 64.29, Anhydrous) (0.149 g, 0.5 mmol), $PdCl_2$ (0.0886 g, 0.5 mmol) and $NiCl_2$ (STREM Chemical, Inc., 99.9%, Anhydrous) (0.0648 g, 0.5 mmol), $PdCl_2$ (0.0886 g, 0.5 mmol), and $AuCl_3$ (STREM Chemical, Inc., 99.9%, Anhydrous) (0.151 g, 0.5 mmol), and $PdCl_2$ (0.0886 g, 0.5 mmol) and AgCl (STREM Chemical, Inc., 99.9%, Anhydrous) (0.0716 g, 0.5 mmol) in 100 ml THF respectively. Almost complete dissolution of the salt(s) occurred after stirring the deep dark coloured solution for 4 h. To destroy any unreacted reducing agent, 5 ml of acetone were added and stirred for 1 h. The solution then was added dropwise to a stirred suspension of the carbon support (Vulcan XC72R) in 100 ml THF. The mixture was stirred for 12 h. 150 ml of ethanol (Sigma-Aldrich, 99.5%, Anhydrous) were then added and stirred for 2 h. After filtering the reaction solution through a D-4 glass frit, the supported catalyst(s) was washed with ethanol several times, and then dried under a nitrogen vacuum at 296 K for 12 h.

Annealing and reducing processes were performed to remove the protective shell in order to enhance the catalytic activity [18-20]. The processes were performed in three stages using a controlled tubular furnace (LINDBERG). First, the samples were heated up to 300°C for 30 min under N_2 (5, BOC Gas) at a flow rate of 160 ml min^{-1}. In this stage most of the organic shell is decomposed. Second, the samples were annealed under a N_2/O_2 (5, BOC Gas) mixture (10 vol.% O_2) at a flow rate of 160 ml min^{-1} for 30 min at 300°C. Third, the samples were reduced under 100 vol.% H_2 at a flow rate of 160 ml min^{-1} for 30 min at 300°C, in order to reduce any oxidized metal(s) formed during the annealing processes. Nitrogen was purged for 5 min before and after the annealing process to avoid any contact between the oxygen and hydrogen gases.

Figure 1 shows the energy dispersive spectroscopy (EDS) spectra

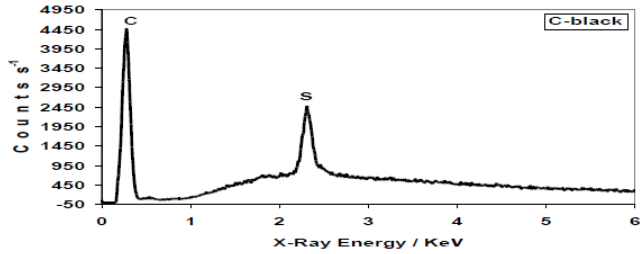

Figure 1. Powder EDS analysis showing the elemental distributions in Vulcan XC72R carbon black.

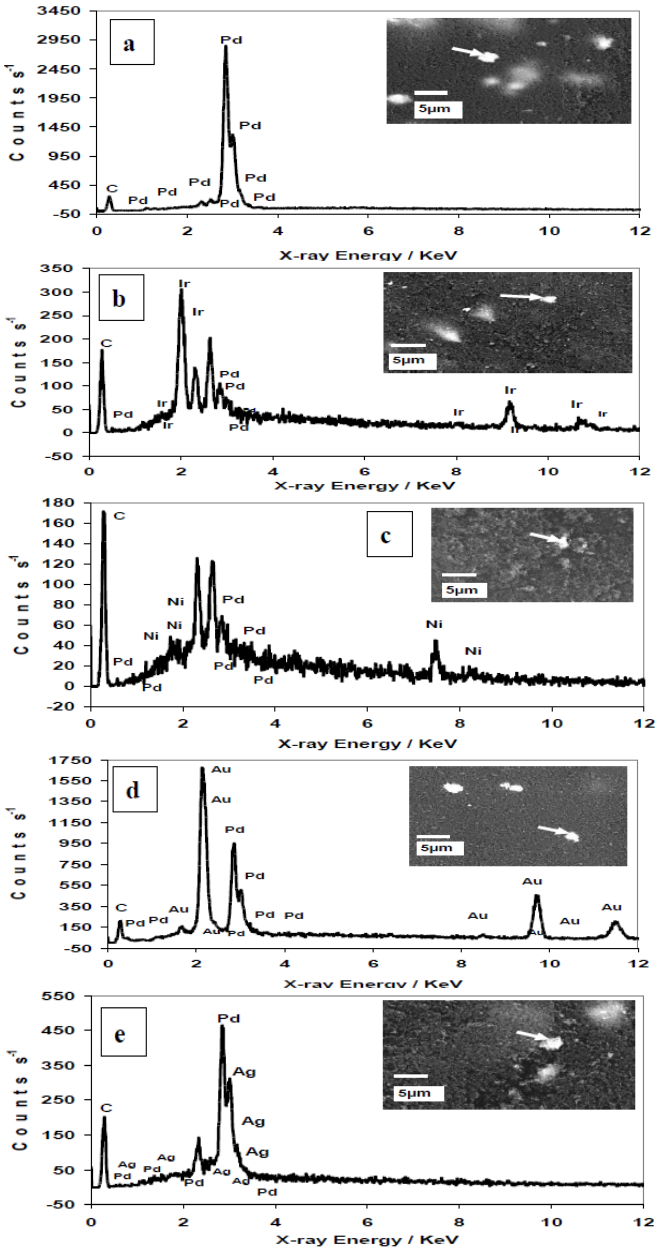

Figure 2. a-e. Powder EDS analysis showing the metal distributions in 20wt% (1:1 atomic ratio) colloidal Pd and Pd-alloys.

for the Vulcan XC72R carbon black, and Figures 2a-e show EDS spectra for the Pd-alloys corresponding to a selected zone in the powder sample as indicated in the SEM micrograph inset. The X-ray diffraction spectra for Vulcan XC72R carbon black and all four catalysts are shown in Figures 3 and 4a-e, respectively. The X-ray diffraction spectra show a remarkable similarity with the base metal (Pd) and all alloys showing a f.c.c. structure.

2.2. Electrode and Cell Preparation for Electrochemical Methods

A glassy carbon disk electrode, 3 mm diameter, manufactured from a glassy carbon rod (Electrosynthesis Inc.), was used as a substrate for the colloidals. Prior to each experiment, the glassy carbon (GC) electrode was polished to a mirror finish first with 1 mm diamond paste and then with 0.05 mm alumina (Cypress System Inc. polishing kit). A thorough washing and ultrasonic cleaning followed the polishing.

To create good bonding of the supported metal colloid catalysts to the GC electrode, 5 mg of the carbon supported catalyst powder (20 % wt metal) was dispersed ultrasonically for 45 minutes in a 1 ml solution composed of 0.25 ml of a Nafion solution 5 % wt (Aldrich) and 0.75 ml of ethanol (Aldrich). From the suspension of the supported catalyst and Nafion, 10 µl was carefully applied on the GC electrode surface yielding for each of the investigated catalysts a constant load per metal basis of 141 µg cm^{-2}. The dispersed catalyst on the GC substrate was dried in a mild N_2 stream for about 1 h creating good bonding and electronic contact between the supported catalyst and the GC electrode.

A conventional three-electrode cell was used to perform the electrochemical tests. The cell was composed of the dispersed colloidal metal GC, two graphite rods with an area of ~ 10 cm^2 acting as the counter-electrode and a Hg/HgO, 2M NaOH (B20B400, Radiometer Analytical S. A.) electrode as the reference electrode with a -0.068 V potential vs. Ag/AgCl, KCl_{std}. (this will be referred to as the MOE). Cyclic voltammetry on static and dynamic electrodes' experiments were carried out in N_2 purged electrolytes at 295 K employing either a PAR 263A or a PARSTAT 2263 computer controlled potentiostat (Princeton Applied Research Inc.) and the associated Power Sweep and Power Step software (part of the Power Suite package). Voltammetry on a rotating disc electrode (RDE) experiments were performed by using Volta Lab 80 (PGZ402, Radiometer Analytical S. A.) in conjunction with the glassy carbon electrode tip (A35T090, Radiometer Analytical S. A.), RDE (EDI101, Radiometer Analytical S. A.), and speed control unit (CTV101, Radiometer Analytical S. A.). For $NaBH_4$ oxidation, 2 M NaOH was used with $NaBH_4$ (Alfa Aesar Inc., purity +97 %wt) concentrations between 0.03 and 1 M.

2.3. Fuel Cell and MEA Preparation

Tests on direct borohydride fuel cells were performed using a Lynntech FCTS MTK system in conjunction with FCPower control software and 5 cm^2 geometric area single fuel cell kits. Membrane electrode assemblies (MEAs) used in this study were prepared in-house by forming and applying the anode side onto a half-MEA with Nafion® 117 membrane supplied by Electrochem Inc. (EC-MEA-C1), where the cathode side consisted of 4 mg Pt cm^{-2} and Toray Carbon paper gas diffusion layer. The anode colloidal catalysts with a metal load of 5 mg cm^{-2} were applied on a carbon cloth

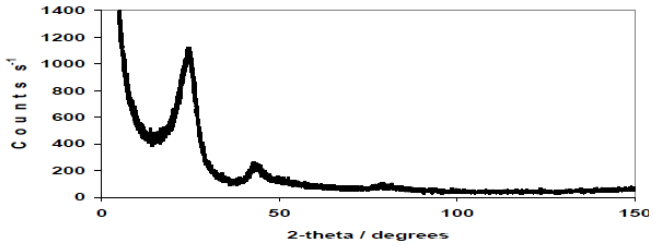

Figure 3. X-ray diffraction pattern of powder Vulcan XC 72R carbon black.

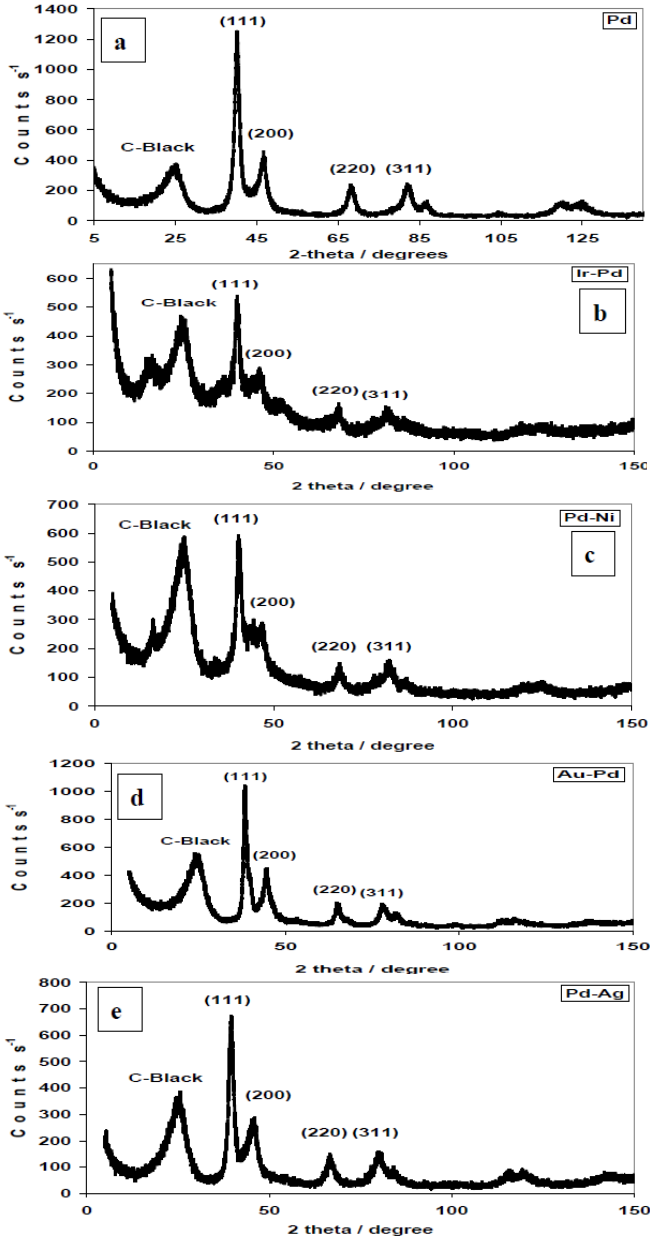

Figure 4. a-e. X-ray diffraction patterns of powder 20wt% (1:1 atomic ratio) colloidal Pd and Pd-alloys, showing [111], [200], [220], and [311] reflections of the fcc lattice of metallic Pd and its alloys.

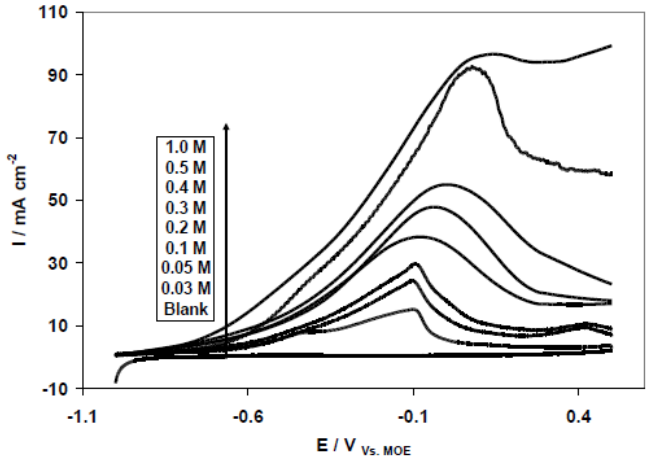

Figure 5. Linear voltammogram of BH_4^- oxidation on colloidal Pd catalyst using a static electrode showing the effect of BH_4^- concentration. Scan rate 100 mV s^{-1}, 298 K. Inset legend indicates the $NaBH_4$ concentration in 2 M NaOH.

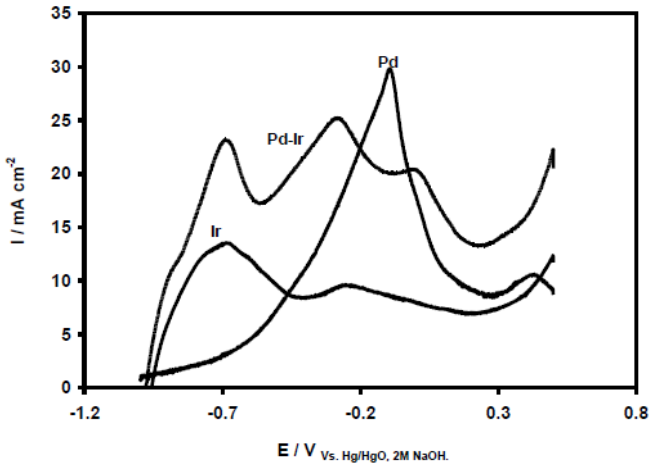

Figure 6. Linear voltammogram of BH4− oxidation on colloidal Pd, Ir, and Pd-Ir catalysts using a static electrode. Scan rate 100 mV s−1, 0.1 M BH4− concentration 298 K.

(ECCC1-060, Electrochem. Inc.). The procedure consisted of the following steps: 5 mg cm^{-2} on metal(s) bases of the colloidal catalyst was mixed with 1 mg cm^{-2} Nafion® 117 (i.e. corresponding volume of Nafion 5%wt solution) and 0.7 ml ethanol. The mixture was sonicated for 45 minutes. Afterwards, the supported catalyst suspension was applied on the carbon cloth by a technique similar to a decal method, followed by drying in a N_2 atmosphere for 12 h. The final stage in the MEA preparation was the hot pressing of the anode catalyst on the carbon cloth substrate, together with another carbon cloth acting as the anodic backing layer onto the Nafion® 117 membrane. Hot pressing was performed at 1200 lb for 2 min at 160ºC.

After the hot pressed full MEA was assembled together with the end plates in the fuel cell test station, membrane conditioning was performed by recirculating a solution of 2 M NaOH at 60 ml min^{-1} for 2 h prior to each test. The pure sodium hydroxide solution was

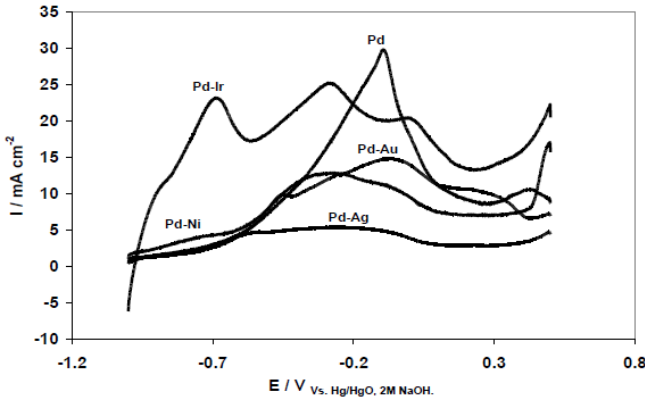

Figure 7. Linear voltammogram of BH_4^- oxidation on colloidal Pd and Pd-alloy catalysts using a static electrode. Scan rate 100 mV s^{-1}, 0.1 M BH_4^- concentration 298 K.

then replaced by a 2 M $NaBH_4$ in 2 M NaOH solution at feed at rates of 20, 50, and 85 ml min^{-1}. The oxygen flow rate was fixed at 0.2 l min^{-1} for all tests, with a gauge pressure of 25 psi. The tests were started after the fuel cell temperature and the fuel feed flow stream temperatures reached either 298 K or 333 K. Potential vs. current data were recorded.

3. RESULTS AND DISCUSSIONS

3.1. Voltammetry of Borohydride Oxidation on Static Electrodes

The linear voltammograms on static electrodes for the colloidal Pd catalyst are shown in Fig. 5, were recorded at scan rate of 100 mV s^{-1} and 0.03-1.0 M $NaBH_4$ concentration in 2 M NaOH.

One oxidation peak can be identified on colloidal Pd between –0.1 and +0.1 V vs. mercury-mercury oxide reference electrode (MOE). This peak slightly shifts to a more positive potential with increasing $NaBH_4$ concentration.

Pd is considered as one of Pt active surface family which are widely used for complete oxidation and hydrogenation-dehydrogenation processes. Therefore, in attempt to enhance its catalytic activity towards BH_4^- oxidation, we decided to investigate the effect of alloying Pd with the same family elements, Ni; with a metal having many free electrons, Ir; and with elements that behave as virtually inert for hydrogenation-dehydrogenation processes, Au and Ag [21].

The effect of alloying Pd with Ir on BH_4^- oxidation is shown in Figure 6. The linear voltammogram of $NaBH_4$ on Pd, Ir, and Pd-Ir catalysts, were recorded at a scan rate of 100 mV s^{-1} and 0.1 M $NaBH_4$ concentration in 2 M NaOH.

Multiple oxidation peaks occurred at around -0.65, -0.25, and between 0 and 0.1 V vs. MOE as a result of alloying with Ir. The peak at –0.65 V, which seems to be associated with Ir, is due to H_2 oxidation and the ones at –0.25 V and around 0 V correspond to direct BH_4^- oxidation on the Ir and Pd surfaces, respectively.

The linear voltammograms on static electrodes for colloidal Pd, Pd-Ir, Pd-Ni, Pd-Au, and Pd-Ag catalysts as shown in Fig. 7, were recorded at scan rate of 100 mV s^{-1} and 0.1 M $NaBH_4$ concentration in 2 M NaOH.

On Pd-Ni, taking into account that there was no peak recorded on

Table 1. Oxidation peak potential, apparent Tafel slopes, exchange current densities, determined from RDE data using supported colloidal Pd and Pd-alloys catalysts with Nafion 117 polymer electrolyte.

Catalysts	Oxidation Peak Potential (V)	b_a ($V.dec^{-1}$) 298 K	$i_{0,a}$ ($A.cm^{-2}$) 298 K
Pd	-0.09	0.787	0.939×10^{-3}
Pd-Ir	-0.34	0.757	13.06×10^{-3}
Pd-Ni	-0.02	0.761	0.765×10^{-3}
Pd-Au	0.00	0.938	0.120×10^{-3}
Pd-Ag	-0.04	0.934	1.670×10^{-3}

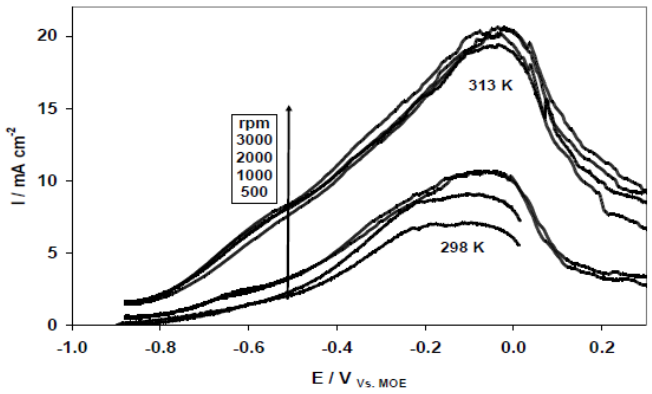

Figure 8. Linear voltammetry of BH_4^- oxidation on colloidal Pd catalysts using a rotating electrode showing the effect of rotation speed and temperature. Scan rate 5 mV s^{-1}, 298 K and 313 K. $NaBH_4$ concentration 0.3 M in 2 M NaOH. Inset legend indicates the rotation speed per minute.

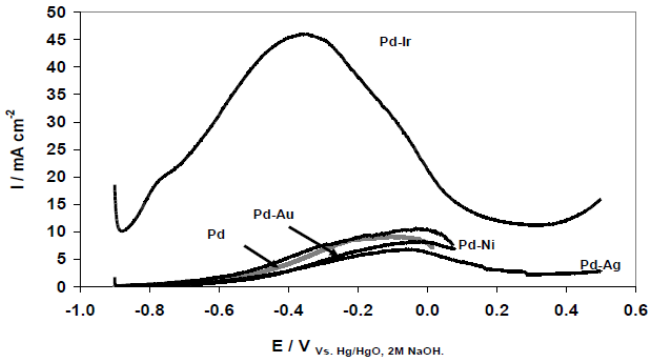

Figure 9. Linear voltammetry of BH_4^- oxidation on colloidal Pd and Pd-alloys catalysts using a rotating electrode showing the effect of alloying. Scan rate 5 mV s^{-1}, 298 K, $NaBH_4$ concentration 0.3 M in 2 M NaOH, and 1000 rpm.

a pure Ni colloidal (no voltammogram shown), two oxidation peaks were observed, one between -0.7 to -0.6 which accounts as alloying action, and the second between -0.25 to 0.1 V vs. MOE. It is worth noting that Kinjo [22], in his investigation of the oxidation of 0.1

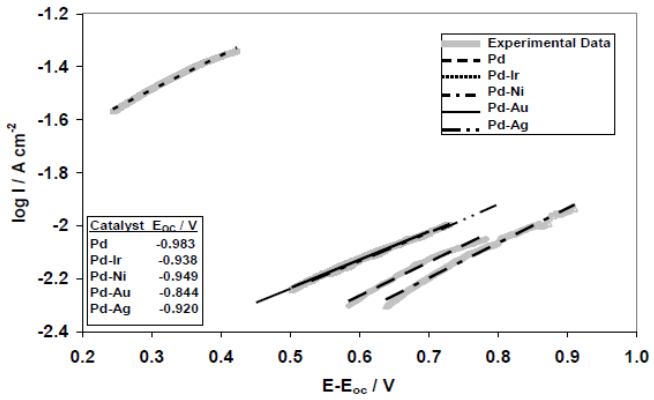

Figure 10. Tafel plots for the supported colloidal Pd and Pd-alloys catalysts generated from the rotating disk electrode data. 298 K.

M KBH_4 in 0.1 M KOH on deposited Pd on porous sintered Ni, recorded three peaks at -0.3, -0.07, and 0.1 V vs. MOE, proposing H_2 gas evolution due to BH_3OH^- oxidization in a three electron process.

For Pd-Au, two oxidation peaks were observed, one between -0.5 to -0.3, and the other around 0 V vs. MOE.

On Pd-Ag, again two oxidation peaks were observed, but one was between -0.55 to -0.4, and the other was between -0.2 to 0 V vs. MOE.

3.2. Voltammetry of Borohydride Oxidation on Rotating Electrodes

The RDE results for colloidal the Pd catalyst, are shown in Figure 8. The scan rate was 5 mV s^{-1}, while the rotation rate was varied between 500 and 3,000 rotations per minute (rpm). The BH_4^- concentration was constant at 0.3 M. Strong temperature and weak rotation effects can be clearly seen. The peak potential on Pd was around 0 V at both 298 K and 313 K, and varied slightly with rotation rate.

Figure 9 shows the linear voltammograms of BH_4^- oxidation on colloidal Pd and Pd-alloy catalysts using a rotating disc electrode (RDE). The scan rate was 5 mVs^{-1}, while the rotation rate was 1000 rotations per minute (rpm). The BH_4^- concentration was constant at 0.3 M. However, on Pd-Ir the peak occurred at more negative potentials, around -0.4 V, at 298 K. For Pd-Ni, Pd-Au and Pd-Ag gave a peak inexactly the same range as for pure Pd.

A plot of log*i* vs. η (=E-E_{OC}) was made according to the Tafel equation, $\eta = b\log\frac{i}{i_o}$ [23], using the rising domains of Fig. 9. This enabled the calculation of both the apparent Tafel slopes and the exchange current densities (Fig. 10).

The apparent Tafel slopes (b_a) are summarised in Table 1 and were in the range of about 0.761 to 0.938 V at 298 K. It is shown that porous electrodes are characterized by so called multiple Tafel slopes due to ionic conductivity and/or mass transfer limitations coupled with electrode kinetics [24, 25].

Alloying Pd with Au and Ag increases the apparent Tafel slope at 298 K, while it decreases when Pd is alloyed with Ni and Ir. The exchange current density at 298 K, on the other hand, increased by 13 times with the addition of Ir (Table 1). Thus, alloying with Ir

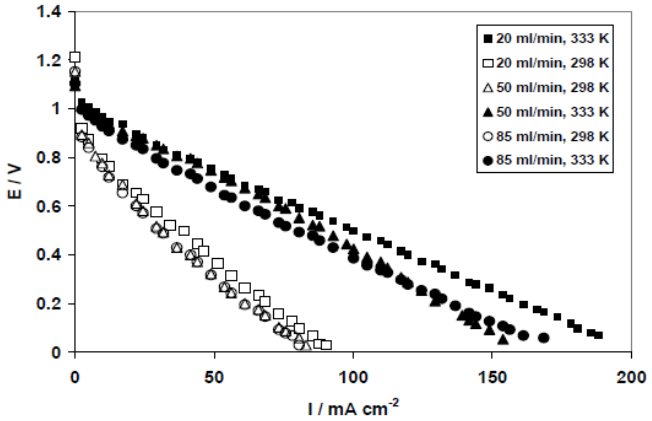

Figure 11. Direct borohydride fuel cell polarization curves of colloidal Pd catalysts at different 2 M $NaBH_4$ – 2 M NaOH fuel flow rates and at 298 K and 333 K. Anode catalyst load 5 mg cm^{-2}. Cathode catalyst (Pt) load 4 mg cm^{-2}. O_2 flow rate 200 ml min^{-1} at 2.7 atm.

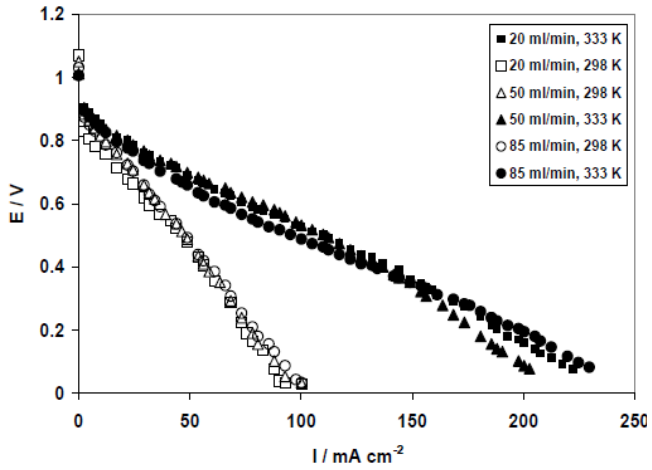

Figure 12. Direct borohydride fuel cell polarization curves of colloidal Pd-Ir catalysts at different 2 M $NaBH_4$ – 2 M NaOH fuel flow rates and at 298 K and 333 K. Anode catalyst load 5 mg cm^{-2}. Cathode catalyst (Pt) load 4 mg cm^{-2}. O_2 flow rate 200 ml min^{-1} at 2.7 atm.

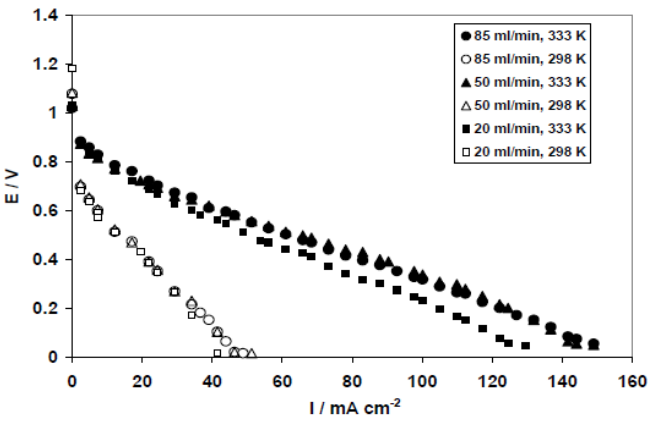

Figure 13. Direct borohydride fuel cell polarization curves of colloidal Pd-Au catalysts at different 2 M $NaBH_4$ – 2 M NaOH fuel flow rates and at 298 K and 333 K. Anode catalyst load 5 mg cm^{-2}. Cathode catalyst (Pt) load 4 mg cm^{-2}. O_2 flow rate 200 ml min^{-1} at 2.7 atm.

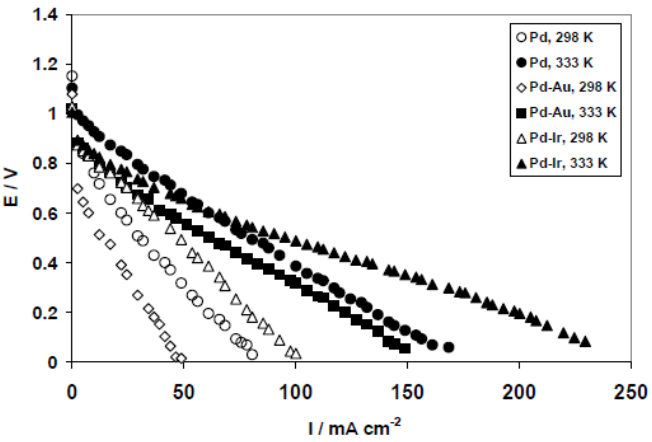

Figure 14. Direct borohydride fuel cell polarization curves at 298 K and 333 K: Comparison between the colloidal catalysts prepared in the present work (Pd, Pd-Ir, and Pd- Au). Anode catalyst load 5 mg cm^{-2}. 50 ml min^{-1} 2 M $NaBH_4$ – 2 M NaOH. Cathode catalyst (Pt) load 4 mg cm^{-2}. O_2 flow rate 200 ml min^{-1} at 2.7 atm.

enhances the activity, since it slightly lowers the Tafel slope and significantly increases the exchange current density [26, 27]. This is in agreement with our previous finding that "the most active catalyst is the one that shows the most negative oxidation peak potential" [28].

3.3. Fuel Cell Performance

Tests on direct borohydride fuel cell (DBFC) were performed for three different flow rates at 298 K and 333 K, using a single cell of 5 cm^2 surface area.

Figures 11-13 show the temperature and fuel flow rate effects on the polarization curves obtained using the colloidal Pd, Pd-Ir, and Pd-Au as anode catalysts respectively. Temperature has a significant impact on the fuel cell performance for all the investigated cases, while the flow rate has no significant effect on the fuel cell performance.

Figure 14 shows a comparison of the fuel cell performance using either colloidal Pd, Pd-Au, or Pd-Ir as anode catalyst. Pd-Ir is the most active electrocatalyst, and a fuel cell employing such an anode catalyst operates at a cell voltage of 0.5 V and gives a current density of 50 mA cm^{-2}. At 333 K, the same catalyst gives 100 mA cm^{-2} at a 0.5 V cell voltage.

Figure 15 shows a comparison between the fuel cell performance using a commercial Pt-Ru or the colloidal Pd, Pd-Au, Pd-Ir alloys as anode catalysts. It is quite clear that fuel cell performance with both Pd and Pd-Ir as the anode catalyst is superior to that with commercial Pt-Ru at 298K.

It should be emphasised that a borohydride fuel cell utilizing Pd-Ir as the anode catalyst can give almost three times a higher power

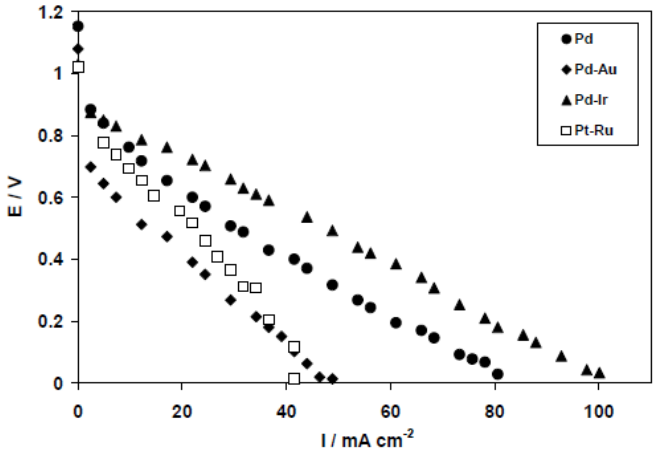

Figure 15. Direct borohydride fuel cell polarization curves at 298 K: Comparison between commercial colloidal Pt-Ru and colloidal catalysts prepared in the present work (Pd, Pd-Ir, and Pd- Au). Anode catalyst load 5 mg cm^{-2}. 50 ml min^{-1} 2 M $NaBH_4$ – 2 M NaOH. Cathode catalyst (Pt) load 4 mg cm^{-2}. O_2 flow rate 200 ml min^{-1} at 2.7 atm.

density (50 mA cm^{-2} at 0.5 V) than that utilizing a commercial Pt-Ru catalyst (17 mA cm^{-2} at 0.5 V) at the same catalyst loading and operating conditions.

4. CONCLUSIONS

The borohydride oxidation catalytic activities of supported Pd and Pd-alloy colloidal nano-particles have been investigated. Colloidal Pd-Ir and Pd were the most active of the investigated electrocatalysts.

CV studies showed that Pd-Ir has the most negative oxidation peak potential. RDE data analysis showed that the b_a values were lower for Pd-Ir followed by Pd-Ni and pure Pd. The highest i_o value was recorded for Pd-Ir.

Fuel cell results showed that Pd-Ir, followed by Pd, were the most active electro- catalysts toward the oxidation of borohydride, since both showed a low b_a and a high i_o which are two key characteristics of a good electrocatalyst.

5. ACKNOWLEDGEMENTS

The authors would like to thank the Natural Science and Engineering Research Council of Canada for their financial support of this work. They would also like to thank Dr. Charles Macdonald (Department of Chemistry and Biochemistry, University of Windsor) for the provision of laboratory facilities for the preparation of the electrocatalysts.

6. REFERENCES

[1] Y. Zhu1, S. Ha, R. Masel, J. Power Sources, 130, 8 (2004).
[2] S. Suda et al., Material Stage, Oct. 10, 1(7), 14 (2001). (www.kucel.hydrogen.co.jp/1-6).
[3] C. Ponce de Leon, F.C. Walsh, D. Pletcher, D.J. Browning, J.B. Lakeman, J. of Power Sources, 155, 172 (2006).
[4] Z.P. Li, B.H. Liu, K. Arai, S. Suda, J. of Alloys and Compounds, 404-406, 648 (2005).
[5] C. Rice, S. Ha, R. I. Masel, A. Wieckowski, J. Power Sources, 155(2), 299 (2003).
[6] K. Yamada, K. Yasuda, H. Tanaka, Y. Miyazaki, T. Kobayashi, J. Power Sources, 122, 132 (2003).
[7] R. Jasinski, Electrochemical Tech., 391, 40 (1965).
[8] S. C. Amendola, P. Onnerud, M. T. Kelly, P. J. Petillo, S. L. Shap-Goldman, M. Binder, J. Power Sources, 84, 130 (1999).
[9] Z. P. Li, B. H. Liu, K. Arai, S. Suda, J. Electrochem. Soc., 150(2), A868 (2003).
[10] Z. P. Li, B. H. Lin, K. Aria, N. Morigazaki, S. Suda, J. Alloys and Comp., 356-357, 469 (2003).
[11] J. Kim, H. Kim, Y. Kang, M. Song, S. Rajendran, S. Han, D. Jung, J. Lee, J. Electrochem. Soc., 151(7), A1038 (2004).
[12] E. Gyenge M. Atwan, , D. Northwood, J. Electrochem. Soc., 153(1), A150 (2006).
[13] M. H. Atwan, C. L. B. Macdonald, D. O. Northwood, E. L. Gyenge, J. Power Sources, 158(1), 36 (2006).
[14] M. H. Atwan, D. O. Northwood, E. L. Gyenge, Inter. J. Hydrogen Energy, 32(15), 3116 (2007).
[15] M. H. Atwan, D. O. Northwood, E. L. Gyenge, Inter. J. Hydrogen Energy, 33(8), 2126 (2008).
[16] H. Bönneman, W. Brijoux, R. Brinkmann, E. Dinjus, T. Joußen, B. Korall, Angew. Chem. Int. Engl., 30(10), 1312 (1991).
[17] M. Götz and H. Wendt, Electrochim Acta 43(24), 3637 (1998).
[18] R. Richards, R. Mortel, H. Bonnemann, Fuel Cell Bulletin, 4(37), 7 (2001).
[19] H. Bönneman, private communication, October 16, (2003).
[20] H. Bönneman, U. Endruschat, J. Hormes, G. Kohl, S. Kruse, H. Modrow, R. Mortel, K.S. Nagabhushana, Fuel Cells, 4(3), 297 (2004).
[21] R. I. Masel, Chemical Kinetics and Catalysis, Wiley-Interscience, NY, 689-755, 837-880, 667-743 (2001).
[22] A. Kinjo, Diss. Abstr. B, 29, 3235 (1969), and Chem. Abstr. 71, 18189 (1969).
[23] A.J. Bard, L. Faulkner, "Electrochemical methods", Wiley, New York, 1980.
[24] M.L. Perry, J. Newman and E.J. Cairns, J. Electrochem. Soc. 145**,** 5 (1998).
[25] J. O'M. Bockris and S.U. M. Khan, "Surface electrochemistry: A molecular level approach", Plenum Press, New York, 1993, P. 280-283, 621.
[26] E. Gileadi, "Electrode Kinetics", VCH, NY, 1993, p. 403-454.
[27] S. H. Jordanov, P. Paunovic. O. Popovski, A. Dimitrov, D. Slavkov, Bull. Chem. Tech. of Macedonia, 23 (2), 101 (2004).
[28]M. H. Atwan, E. L. Gyenge, D. O. Northwood, "Electrochemical Evaluation of Electro catalysts for Fuel Cell Applications: A Practical Approach", Invited paper Presented at the International Symposium on Solar-Hydrogen-Fuel Cells-10 (International Materials Research Congress 2006), Cancun, Mexico, August 20-24, 2006.